

基于透明超声换能器的光声显微镜设计

何勇¹, 廖唐云¹, 吴俊伟^{1,3}, 邓丽军^{1,2}, 邓宇³, 曾吕明^{1,2*}, 纪轩荣¹

¹广东工业大学精密电子制造技术与装备国家重点实验室, 广东 广州 510006;

²江西科技师范大学江西省光电子与通信重点实验室, 江西 南昌 330038;

³广州多浦乐电子科技股份有限公司, 广东 广州 510530

摘要 光声显微镜结合了光学成像的高分辨率和声学成像的组织穿透深度, 在生物医学领域有着广泛的应用。随着技术的发展, 其小型化系统有着新的发展机遇。然而, 传统光声显微镜的光路受超声换能器的不透明影响, 声-光共聚焦扫描需要复杂的模块, 不利于光声系统的小型化发展。提出了基于透明超声换能器的光声显微镜, 自主制作了 7 MHz 透明超声换能器, 实现了小型化、低成本、大视场的同轴共焦成像模式。实验结果表明: 基于透明超声换能器的光声显微镜, 横向分辨率为 18.0 μm , 信噪比高达 38 dB, 成像范围可达 16 mm \times 16 mm。对小鼠鼠耳皮下血管的成像实验验证了系统具有成像生物组织网络的能力。

关键词 医用光学; 超声换能器; 光声显微镜; 生物医学应用; 小型化; 大视场

中图分类号 O426

文献标志码 A

doi: 10.3788/CJL202249.0307001

1 引言

光声显微镜在生物医学领域的应用广泛, 如从单个细胞到器官的跨尺度成像、无标记的功能成像以及使用外源性造影剂的分子成像等^[1-3]。光声显微镜在各领域取得了丰富的研究成果, 如血管生物学、组织学、肿瘤学、神经科学和眼科等^[4-9]。光声显微镜可以分为光学分辨光声显微镜和声学分辨光声显微镜, 均采用光学聚焦区域与声学聚焦区域重合的办法来获取最佳的信噪比。其中, 光学分辨光声显微镜的聚焦光斑直径小于接收换能器的声焦点直径, 在系统的横向分辨率上, 光学分辨光声显微镜更具优势, 这由聚焦区域较小的焦点直径决定, 达到衍射极限的光斑直径可使系统具有亚微米级的横向分辨率^[10-13]。

传统的光声显微镜往往体积大, 集成度低, 使用和维护成本高, 使用人员需要具备较为专业的能力。随着技术的进步, 光声显微镜有向小型化发展的趋

势, 如手持式、穿戴式、便携式等^[14-16]。系统小型化包括光声成像系统的整体优化和具体物理系统的小型化, 如扫描光路精简的小型化、二维扫描振镜的小型化以及超声换能器的小型化等。小型化的光声显微镜具有集成度更高、体积更小、应用范围更广等特点^[17-19]。然而, 传统的光学分辨光声显微镜由于超声换能器阻碍光的传播, 要达成光声同轴聚焦需要复杂的模块, 不利于系统的小型化。传统光声显微镜可以通过多种方式来实现光声同轴聚焦^[20-22], 比如使用棱镜组合器, 激光通过棱镜改变传播路径, 与超声换能器实现同轴聚焦; 或使用环形超声换能器, 激光通过环形超声换能器中心孔照射在样品上, 由此实现光声同轴聚焦。此外, 还可以通过光纤换能器来接收激光照射在样品上产生的光声信号。虽然通过不同的途径实现了光声信号采集, 但同时也限制了系统的成像速度和成像范围, 还可能增加系统的复杂程度。因此, 寻找更便捷的光声同轴聚焦方式对光声显微镜性能的提高和小型化发展具有重要

收稿日期: 2021-04-30; 修回日期: 2021-05-25; 录用日期: 2021-06-18

基金项目: 广东省珠江人才计划(2016ZT06G375)、国家自然科学基金(11664011, 11804059)、江西省自然科学基金(20171ACB20027)、2017 年度南昌市洪城计划

通信作者: *zenglvming@163.com

的意义。

基于透明换能器的光声显微镜利用透光性较好的 LiNbO_3 材料,以更便捷的方式实现光声同轴聚焦^[23-25]。Dangi 等^[26-27]提出了基于透明换能器的光声显微镜,制作的透明换能器的中心频率为 13 MHz,窗口尺寸仅为 10 mm×10 mm,但采用的传统机械的栅格扫描方式限制了系统的成像范围和扫描速度。为了实现更大的扫描视场和更快的扫描速度,本文制备了更大尺寸的透明换能器,并结合快速的激光振镜扫描,单次成像范围最大可达 16 mm×16 mm,适用于大范围的组织和器官成像,比如小鼠大脑和皮下肿瘤等。

2 实验装置和成像系统

图 1(a) 所示为本实验室自主研制的基于 LiNbO_3 的透明超声换能器照片,其外形尺寸为 33 mm×33 mm,高 10 mm,中心透光窗口的尺寸

为 20 mm×20 mm。其制作流程如下:首先准备一片 36° Y 切的透明 LiNbO_3 单晶作为基板,并将其切割成 20 mm×20 mm 的方形;随后通过光学晶体研磨工艺,将切割好的 LiNbO_3 单晶研磨至厚度为 540 μm ;采用物理气相沉积(PVD)方法,在透明 LiNbO_3 单晶晶片两侧分别沉积一层厚度为 200 nm 的透明铟锡氧化物(ITO)作为顶部和底部电极,并采用微型银绞线将这两个电极连接至 BNC (Bayonet Nut Connector);采用一个定制的方形金属外壳对透明换能器进行保护封装,外壳和 LiNbO_3 单晶之间的间隙用不导电的透明环氧树脂填充;最后在换能器的顶部再沉积一层 66 μm 厚的透明环氧树脂作为声学匹配层。目前, LiNbO_3 晶体的生长极限为 150 mm,这是透明换能器能达到的最大尺寸。通过对加工工艺和制作技术进行优化,能制作出更高频、窗口尺寸更大的透明超声换能器,其性能得到进一步提升。

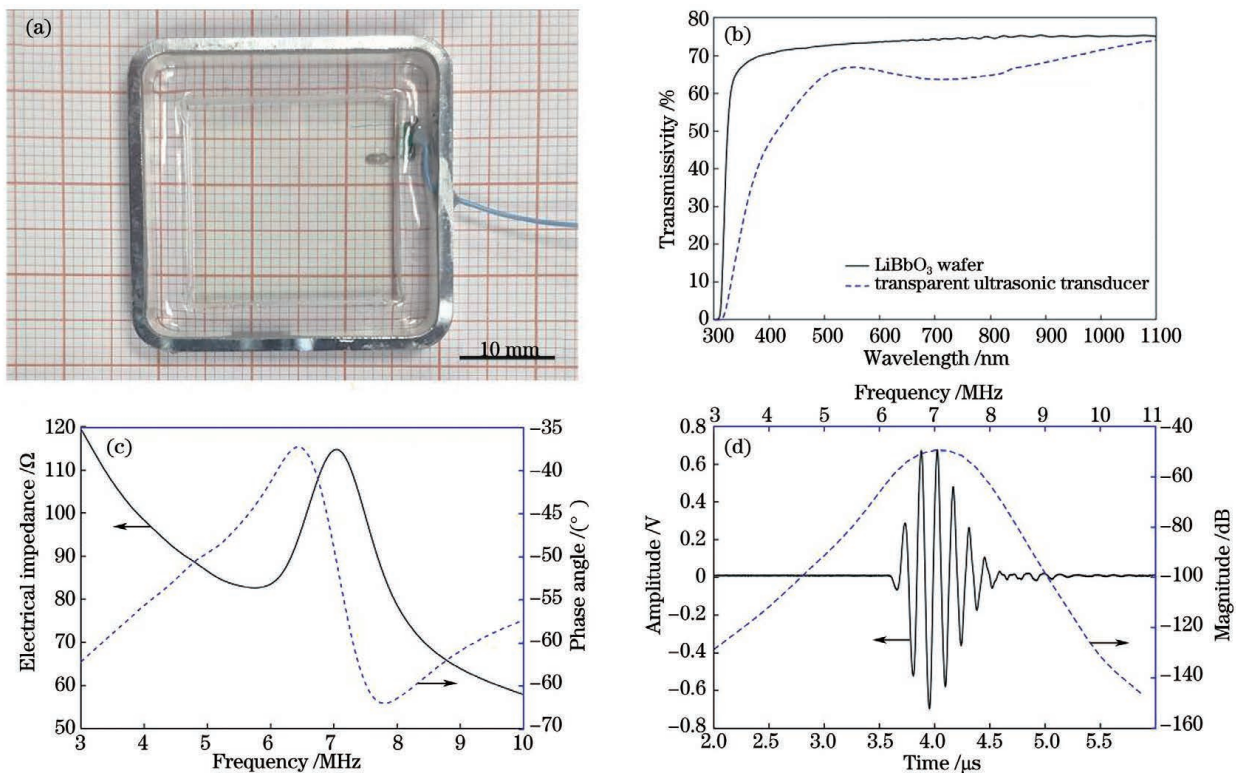


图 1 透明超声换能器的性能表征。(a) 7 MHz 铌酸锂透明超声换能器的实物图;(b)透光曲线;(c)电阻抗和相位角;(d)脉冲回波曲线及频谱

Fig. 1 Performance characterization of transparent ultrasonic transducer. (a) Physical image of 7 MHz LiNbO_3 transparent ultrasonic transducer; (b) light transmittance curves; (c) electrical impedance and phase angle; (d) pulse echo curve and spectrum

我们对所制作出的透明换能器进行了一系列的性能测试实验。图 1(b)所示为 LiNbO_3 单晶以及基于 LiNbO_3 的透明换能器对不同波长光的透射

率,可以看到,对于可见光波段,所制作的透明换能器在 532 nm 处的透射率最高,达到了 66.55%。本文计划对生物组织皮下微血管网络进行成像研究,

而生物组织中的血红蛋白在 532 nm 附近的光学吸收率比近红外波段的光学吸收率高 1 个数量级以上。因此,本文选用 532 nm 波长的激光作为光源,可获得更高的灵敏度和信噪比。在后续工作中,也可匹配近红外波段的外源性造影剂进行光声成像。随后我们测试了该透明换能器的阻抗谱和相位角谱,如图 1(c) 所示,可以看到,换能器的共振频率(f_r)和谐振频率(f_a)分别为 5.80 MHz 和 7.03 MHz,由此可计算得到换能器的机电耦合系数(K_{eff})约为 0.72。对换能器进行了脉冲回波测试实验,测得该透明超声换能器的中心频率为 7 MHz, -6 dB 分数带宽为 25.66%,如图 1(d) 所示。在后续工作中,通过增加高声衰减和高透光率的背衬层并优化匹配层等,可进一步提升换能器的带宽等性能。

我们所搭建的基于透明超声换能器的光声显微

镜的系统结构示意图如图 2(a) 所示。一个 532 nm Nd:YAG 激光器作为系统的光源并产生重复频率为 5 kHz 的脉冲激光。激光分别经过光阑(Iris)和中性密度过滤器(NDF),进行光束整形和能量衰减后进入二维振镜扫描系统,并被振镜引导着对成像样品进行光栅式扫描。系统采用一个扫描透镜作为聚焦镜对入射激光进行紧密聚焦,聚焦后的激光穿过透明超声换能器照射在成像样品表面。透明换能器被安装在一个定制的水槽的底部,水槽顶部开有一个成像窗口并用薄的聚乙烯薄膜密封,水槽中填充去离子水作为耦合介质。从样品中激发出的光声信号被透明超声换能器检测到,并被信号放大器放大以及高速数据采集卡采集,然后被传输至高性能计算机进行处理成像。系统中激光出光、振镜扫描以及数据采集触发的同步由一块模拟电压输出卡控制。

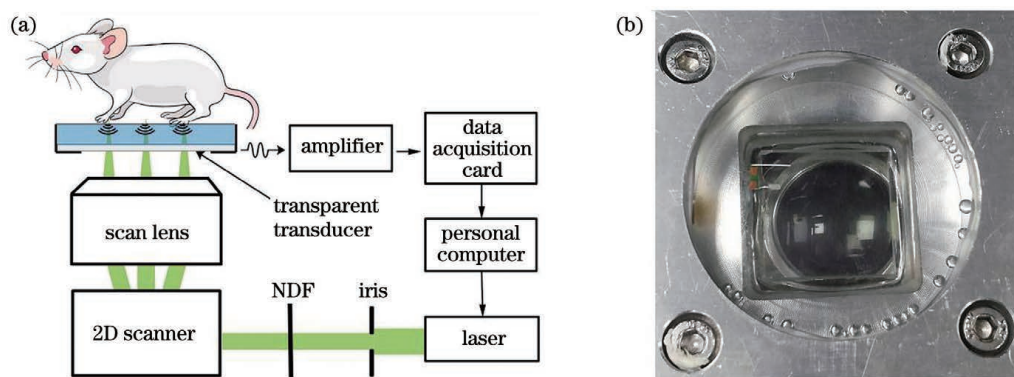


图 2 基于透明超声换能器的光声显微镜系统。(a)结构示意图;(b)成像头的俯视图

Fig. 2 Photoacoustic microscope system based on transparent ultrasonic transducer. (a) Structural diagram; (b) top view of image head

3 实验方法及结果

3.1 系统成像性能检测

我们所采用的聚焦透镜是一款扫描透镜,其最

小光斑尺寸可以达到 $11 \mu\text{m}$,这可以认为是系统的理论横向分辨率。为了评估我们所搭建的光声显微镜系统的实际分辨率,使用该显微镜对刀刃锋利边缘进行了光声成像实验,成像结果如图 3(a) 所示。

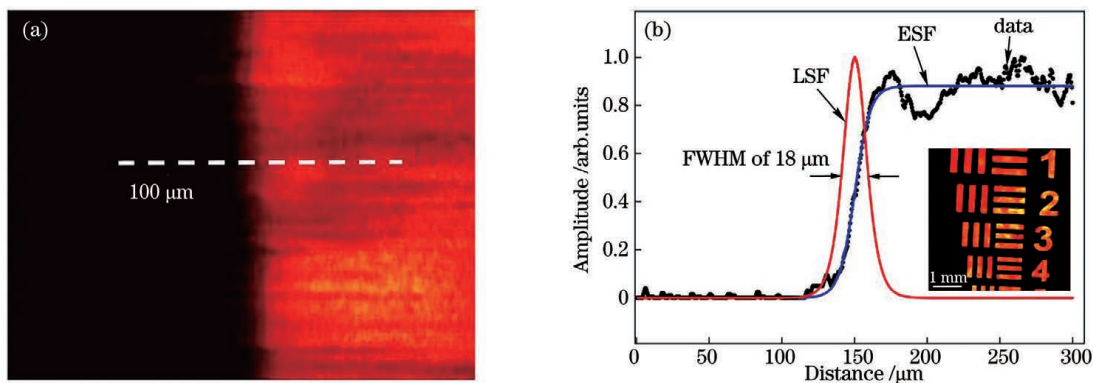


图 3 系统分辨率测试。(a)刀刃锋利边缘的光声图;(b)系统的横向分辨率

Fig. 3 Test of system resolution. (a) Photoacoustic image of blade sharp edge; (b) lateral resolution of system

沿图 3(a)中的虚线获取图像的边缘响应函数,如图 3(b)中 data 曲线所示。对该边缘响应函数进行拟合,得到边缘扩展函数(ESF),再对边缘扩展函数进行一阶求导,获得线扩展函数(LSF)。通过测量线扩展函数的半峰全宽(FWHM),可知系统的实际成像横向分辨率约为 $18 \mu\text{m}$,并对光学分辨率板进行了成像验证,展示了其对生物组织微血管网络成像的能力。在后续的研究工作中,我们将采用具有更小聚焦光斑尺寸的聚焦透镜来进一步提高系统的横向分辨率。

3.2 模拟样品的光声图像

为了进一步评估我们的光声显微镜系统的成像性能,分别对直径约为 $7 \mu\text{m}$ 的碳纤维丝以及叶脉进行了成像实验。在对碳纤维丝的成像实验中,扫描步距设置为 $5 \mu\text{m}$,扫描范围为 $5 \text{ mm} \times 5 \text{ mm}$ 。图 4(a)和图 4(b)分别展示了碳纤维丝样品的照片和最大幅值光声图像,从光声图像中可以清晰地观察到碳纤维丝交叉与弯曲的结构,与光学照片中的形状结构一致。另提取了样品信号的峰值和噪声信号的均方根,经计算其信噪比(SNR)高达 38 dB。随后我们对大范围的叶脉进行了成像

实验,将制作好的叶脉样品平铺在系统的成像窗口薄膜上,设置系统的扫描步距为 $50 \mu\text{m}$,扫描范围为 $16 \text{ mm} \times 16 \text{ mm}$,在不进行信号平均处理的情况下测得图像获取的时间约为 50 s。大范围叶脉的光声图像如图 4(c)所示,可以清晰地分辨叶脉的主脉和细小的分支结构,验证了本系统具有对尺寸为厘米级的样品进行快速高分辨率成像的能力。图 4(c)中呈现出的圆形范围是由于扫描范围超出了系统所采用的扫描透镜的视场范围,可以通过采用具有更大扫描范围的扫描透镜来解决。为了更清晰地观察叶脉图像中标记区域的微细末端结构,我们采用 $10 \mu\text{m}$ 的步距对 $2 \text{ mm} \times 2 \text{ mm}$ 的小范围区域进行了小步距高精度扫描成像,成像结果如图 4(d)所示,成像时间约为 10 s。可以更加清晰地分辨出在图 4(c)中显示略微模糊的叶脉微细末端结构。当扫描步距为 $20 \mu\text{m}$ 时,若不进行信号平均处理,系统可实现 100 Hz/mm 的成像速度。这意味着本文所搭建的基于透明换能器的光声显微镜可以实现大视场快速筛查与小范围高分辨成像的多模式切换,具有应用不同场景的潜力。

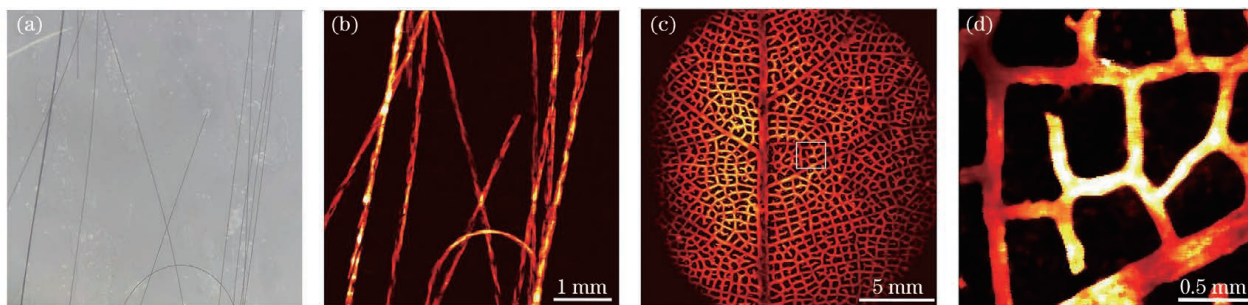


图 4 模拟样品的图像。(a)碳纤维丝的光学图;(b)碳纤维丝的光声图;(c)叶脉骨架的光声图;(d)叶脉骨架局部侧脉的光声图

Fig. 4 Images of simulated sample. (a) Optical diagram of carbon fiber filament; (b) photoacoustic image of carbon fiber filament; (c) photoacoustic image of leaf vein skeleton; (d) photoacoustic image of local lateral veins of leaf vein skeleton

3.3 生物组织的光声图像

对仿体的成像实验已经验证了本文所搭建的光声显微镜系统具有对微细网络状结构样品的成像能力。为了进一步验证系统对生物组织的成像能力,我们设计了一组对离体小鼠耳朵皮下微血管网络的成像实验,小鼠的品种为昆明小鼠,从广州医科大学实验动物中心购得。在进行成像实验之前,需要使用脱毛膏对小鼠耳朵进行脱毛处理,处理好的离体小鼠耳朵照片如图 5(a)所示,从照片中可以看到小鼠耳朵皮下的主要血管网络。对照片中标记的

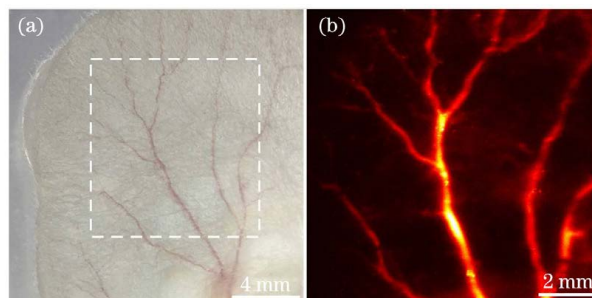


图 5 小鼠鼠耳的图像。(a)光学图;(b)光声图
Fig. 5 Images of mouse ear. (a) Optical image; (b) photoacoustic image

10 mm×10 mm 的区域进行光声成像,扫描步距设置为 20 μm,成像时间测得约为 1 min,成像结果如图 5(b)所示。可以看出,小鼠耳皮下微血管网络结构清晰可见,其血管形态与其照片中的形态一致,证明了该光声显微镜系统具有对生物组织皮下血管的成像能力。实验中透过透明换能器的脉冲激光能量测得为~7 μJ,光学焦点设置在样品表面以下约 1 mm 处,因此计算得到激光的能量密度约为 20.2 mJ/cm²,低于美国国家标准协会(ANSI)的安全极限 22 mJ/cm²。

4 结 论

光声显微镜在生物医学领域具有很好的应用前景,其中小型化光声显微镜有利于成为临床应用的突破口。针对传统光声显微镜在扫描范围和成像速度之间的矛盾及小型化发展的前景,提出了基于透明换能器的光声显微镜,完成了系统的硬件设计、软件开发和仿体实验等一系列工作。在传统光声显微镜的基础上,自主研制了透明超声换能器,对系统光路进行了优化,设计了一套基于透明超声换能器的光声显微镜,系统的横向分辨率为 18 μm,信噪比达 38 dB,兼顾较大的成像视场和较快的成像速度,单次成像范围可达 16 mm×16 mm。系统的激光重复频率为 5 kHz,在扫描步距为 20 μm 时,若不进行信号平均处理,系统可实现 100 Hz/mm 的成像速度。同时,在生物组织成像实验中,血管形态与其照片中的形态一致,表明系统具有在生物医学领域应用的潜力。在后续研究中,将继续完善该系统,开展更多的在体实验,探索该系统在其他生物组织中的应用价值,比如对小鼠脑部皮下微血管和皮下黑色素瘤等进行成像,向临床应用方向转化。

参 考 文 献

- [1] Yao J, Wang L, Yang J M, et al. High-speed label-free functional photoacoustic microscopy of mouse brain in action[J]. *Nature Methods*, 2015, 12(5): 407-410.
- [2] Sathiyamoorthy K, Strohm E M, Kolios M C. Low-power noncontact photoacoustic microscope for bioimaging applications [J]. *Journal of Biomedical Optics*, 2017, 22(4): 046001.
- [3] Cao R, Li J, Ning B, et al. Functional and oxygen-metabolic photoacoustic microscopy of the awake mouse brain[J]. *NeuroImage*, 2017, 150: 77-87.
- [4] Chen Z J, Yang S H, Xing D. Progress and application of photoacoustic microscopy technique [J]. *Chinese Journal of Lasers*, 2018, 45(3): 0307008.
- [5] Lu T, Gao F, Song S Z, et al. Tumor-specific imaging of small animals based on multi-angle optoacoustic mesoscopy imaging method[J]. *Chinese Journal of Lasers*, 2020, 47(2): 0207032.
- [6] Dong B Q, Sun C, Zhang H F. Optical detection of ultrasound in photoacoustic imaging[J]. *IEEE Transactions on Biomedical Engineering*, 2017, 64(1): 4-15.
- [7] Laufer J G, Zhang E Z, Treeby B E, et al. *In vivo* preclinical photoacoustic imaging of tumor vasculature development and therapy[J]. *Journal of Biomedical Optics*, 2012, 17(5): 056016.
- [8] Zeng L M, Piao Z L, Huang S H, et al. Label-free optical-resolution photoacoustic microscopy of superficial microvasculature using a compact visible laser diode excitation[J]. *Optics Express*, 2015, 23(24): 31026-31033.
- [9] Lan B, Liu W, Wang Y C, et al. High-speed widefield photoacoustic microscopy of small-animal hemodynamics[J]. *Biomedical Optics Express*, 2018, 9(10): 4689-4701.
- [10] Wang L V. Tutorial on photoacoustic microscopy and computed tomography[J]. *IEEE Journal of Selected Topics in Quantum Electronics*, 2008, 14(1): 171-179.
- [11] Yao J J, Wang L V. Photoacoustic microscopy[J]. *Laser & Photonics Reviews*, 2013, 7(5): 758-778.
- [12] Yang J, Gong L, Xu X, et al. Motionless volumetric photoacoustic microscopy with spatially invariant resolution[J]. *Nature Communications*, 2017, 8(1): 780.
- [13] Pérez-López S, Fuster J M, Candelas P, et al. On the focusing enhancement of Soret zone plates with ultrasound directional transducers[J]. *Applied Physics Letters*, 2019, 114(22): 224101.
- [14] Liu Q, Jin T, Chen Q, et al. Research progress of miniaturized photoacoustic imaging technology in biomedical field[J]. *Chinese Journal of Lasers*, 2020, 47(2): 0207019.
- [15] Chen Q, Guo H, Jin T, et al. Ultracompact high-resolution photoacoustic microscopy[J]. *Optics Express*, 2020, 28(10): 17800-17810.

- Letters, 2018, 43(7): 1615-1618.
- [16] Lin L, Zhang P F, Xu S, et al. Handheld optical-resolution photoacoustic microscopy [J]. Journal of Biomedical Optics, 2016, 22(4): 041002.
- [17] Huang K, Chen P, Liu W W, et al. Reconstruction for sparse-view sampling photoacoustic signals based on dictionary learning [J]. Acta Optica Sinica, 2018, 38(11): 1117002.
黄凯, 陈平, 刘伟伟, 等. 基于字典学习的稀疏角度采样光声信号重建 [J]. 光学学报, 2018, 38(11): 1117002.
- [18] Dangi A, Agrawal S, Datta G R, et al. Towards a low-cost and portable photoacoustic microscope for point-of-care and wearable applications [J]. IEEE Sensors Journal, 2020, 20(13): 6881-6888.
- [19] Zeng L M, Liu G D, Yang D W, et al. Compact optical-resolution photoacoustic microscopy system based on a pulsed laser diode [J]. Chinese Journal of Lasers, 2014, 41(10): 1004001.
曾吕明, 刘国栋, 杨迪武, 等. 基于脉冲激光二极管的小型化光学分辨式光声显微成像系统 [J]. 中国激光, 2014, 41(10): 1004001.
- [20] Zhou Y Y, Chen J B, Liu C, et al. Single-shot linear dichroism optical-resolution photoacoustic microscopy [J]. Photoacoustics, 2019, 16: 100148.
- [21] Liang Y, Jin L, Guan B O, et al. 2 MHz multi-wavelength pulsed laser for functional photoacoustic microscopy [J]. Optics Letters, 2017, 42(7): 1452-1455.
- [22] Dangi A, Agrawal S, Tiwari S, et al. Evaluation of high frequency piezoelectric micromachined ultrasound transducers for photoacoustic imaging [J]. IEEE Sensors, 2018: 1-4.
- [23] Chen X Y, Chen R M, Chen Z Y, et al. Transparent lead lanthanum zirconate titanate (PLZT) ceramic fibers for high-frequency ultrasonic transducer applications [J]. Ceramics International, 2016, 42(16): 18554-18559.
- [24] Chen Q M, Wang Q M. The effective electromechanical coupling coefficient of piezoelectric thin-film resonators [J]. Applied Physics Letters, 2005, 86(2): 022904.
- [25] Searfass C T, Tittmann B R. High temperature ultrasonic transducer up to 1000 °C using lithium niobate single crystal [J]. Applied Physics Letters, 2010, 97(23): 232901.
- [26] Dangi A, Agrawal S, Kothapalli S R. Lithium niobate-based transparent ultrasound transducers for photoacoustic imaging [J]. Optics Letters, 2019, 44(21): 5326-5329.
- [27] Chen H Y, Agrawal S, Dangi A, et al. Optical-resolution photoacoustic microscopy using transparent ultrasound transducer [J]. Sensors, 2019, 19(24): 5470.

Design of Photoacoustic Microscope Based on Transparent Ultrasonic Transducer

He Yong¹, Liao Tangyun¹, Wu Junwei^{1,3}, Deng Lijun^{1,2}, Deng Yu³, Zeng Lüming^{1,2*},
Ji Xuanrong¹

¹ State Key Laboratory of Precision Electronics Manufacturing Technology and Equipment, Guangdong University of Technology, Guangzhou, Guangdong 510006, China;

² Key Laboratory of Photoelectronics and Telecommunication of Jiangxi Province, Jiangxi Science and Technology Normal University, Nanchang, Jiangxi 330038, China;

³ Doppler Electronic Technologies Incorporated Company, Guangzhou, Guangdong 510530, China

Abstract

Objective Photoacoustic microscope is widely used in the field of biomedicine and has obtained rich research results in various fields. With the development of technologies, the miniaturization of a photoacoustic microscope system has obtained new development opportunities. However, the traditional optically resolved photoacoustic microscope needs complex modules to achieve photoacoustic coaxial focus because the ultrasonic transducer blocks the transmission of light, which is not conducive to the miniaturization of the system. The traditional photoacoustic microscope has achieved photoacoustic signal acquisition through different ways, but it also limits the imaging speed and imaging range of the system and may increase the complexity of the system. The photoacoustic microscope based on a transparent transducer has been developed, in which the window size is less than 10 mm × 10 mm and the raster

scanning mode of traditional machinery is adopted, but the imaging range and scanning speed of the system are limited. In this study, we report a photoacoustic microscope based on a transparent transducer. A larger size transparent transducer is fabricated and combined with fast laser vibroscope scanning to achieve $16\text{ mm} \times 16\text{ mm}$ range in a single imaging, which is suitable for imaging a wide range of tissues and organs, such as mouse brain and subcutaneous tumors.

Methods In this study, firstly, a transparent ultrasonic transducer based on LiNbO_3 is prepared with an external size of $33\text{ mm} \times 33\text{ mm}$, a height of 10 mm , and a central translucent window size of $20\text{ mm} \times 20\text{ mm}$. Then, a photoacoustic microscope based on this transparent ultrasonic transducer is constructed. Third, the lateral resolution of the system is verified by imaging the edge of the blade, and the imaging speed and field of view of the system are verified by imaging the carbon fiber filament and the leaf vein skeleton. Finally, the performance of the system for imaging microvascular network in biological tissue is verified by the mouse ear imaging.

Results and Discussions The test shows that the transparent transducer made in this paper has a good performance (Fig. 1). We perform photoacoustic imaging experiments on the sharp edge of the blade with this microscope, and the actual transverse resolution of the system is about $18\text{ }\mu\text{m}$. We also verify the imaging of the optical resolution plate, demonstrating its ability to image the microvascular network of biological tissue (Fig. 3). In the imaging experiment of carbon fiber, the cross and bend shape structure of a carbon fiber can be clearly observed, and the signal is calculated with a signal-to-noise ratio (SNR) of up to 38 dB . A vein imaging experiment is carried out, verifying that the system can achieve $16\text{ mm} \times 16\text{ mm}$ range in a single imaging (Fig. 4). Finally, the imaging experiment is carried out on the rat ear, in which the structure of the microvascular network under the rat ear skin is clearly visible and the vascular morphology is consistent with that in the photos, which proves that the photoacoustic microscope system has the imaging ability of subcutaneous blood vessels in biological tissues (Fig. 5).

Conclusions In this paper, based on the contradictions among the scanning range, imaging speed of traditional photoacoustic microscope, and the prospect of miniaturization, a photoacoustic microscope based on a transparent transducer is proposed, and a series of works such as hardware design, software development and simulation experiment of the system are completed. On the basis of the traditional photoacoustic microscope, our laboratory independently develops a transparent ultrasonic transducer to optimize the optical path of the system. A set of photoacoustic microscope based on the transparent ultrasonic transducer is designed. The lateral resolution of the system is $18\text{ }\mu\text{m}$ and the signal-to-noise ratio is up to 38 dB , which both give a large imaging field of view and a fast imaging speed. A single imaging can achieve $16\text{ mm} \times 16\text{ mm}$ range. The laser repetition rate of the system is 5 kHz and the imaging speed of 100 Hz/mm can be achieved when the scanning step is $20\text{ }\mu\text{m}$. At the same time, the vascular morphology in the biological tissue imaging experiment is consistent with that in the photos, suggesting that the system has the potential to be applied in the biomedical field. Above all, the photoacoustic microscope based on a transparent transducer can give consideration to both a large imaging field of view and a fast imaging speed, and has a good application prospect in system miniaturization and functional imaging of biological tissues.

Key words medical optics; ultrasonic transducer; photoacoustic microscope; biomedical applications; miniaturization; large field-of-view